

# Ultrahigh-Pressure Melting of Lead: A Multidisciplinary Study

B. K. GODWAL,\* CHARLES MEADE, RAYMOND JEANLOZ,† ALBERTO GARCIA,  
AMY Y. LIU, MARVIN L. COHEN

Measurements of the melting temperature of lead, carried out to pressures of 1 megabar ( $10^{11}$  pascal) and temperatures near 4000 kelvin by means of a laser-heated diamond cell, are in excellent agreement with the results of previous shock-wave experiments. The data are analyzed by means of first principles quantum mechanical calculations, and the agreement documents the reliability of current experimental and theoretical techniques for studies of melting at ultrahigh pressures. These studies have potentially wide-ranging applications, from planetary science to condensed matter physics.

MELTING, THE EQUILIBRIUM TRANSITION BETWEEN CRYSTALLINE and liquid states, is of widespread importance in the physical sciences. For example, some of the highest purity crystals, including silicon, diamond, and others of great technological utility, are grown from the melt (1). At the same time melting, especially at high pressures, is one of the main processes by which the interiors of terrestrial planets evolve, both thermally and by way of geochemical differentiation (2). Despite the broad interest in the subject, there is as yet only a poor understanding of the detailed physical mechanisms by which a crystal melts or a liquid freezes (3). Because of recent advances in experimental and theoretical techniques, however, pressure offers an important thermodynamic variable with which to study the melting process. That is, pressure can be used to systematically alter the interatomic bonding forces and atomic packing configurations of a material such that the resulting effect on the melting temperature can be examined (4).

In the present work we have studied the effect of high pressures on the fusion temperature of elemental lead, a material that could serve as a prototype for other studies of melting at high pressures. The advantages of studying Pb are that (i) its melting temperature at ambient pressures is low and well determined, (ii) it is highly compressible and should therefore readily show the effects of pressure, (iii) the behavior of this metal under pressure is relatively simple, involving only one known polymorphic transition (from

face-centered cubic to hexagonal close-packed crystal structures), and (iv) detailed shock-wave experiments have been previously carried out to document the compression of both crystalline and molten lead at simultaneously high pressures and temperatures (5). Our approach is to extend these prior studies so that the melting of lead is characterized by several independent yet complementary techniques, including the best experimental and theoretical methods currently available for characterizing materials at ultrahigh pressures.

**High-pressure melting experiments on lead.** We carried out experiments with the laser-heated diamond cell, using techniques that have been described before (6, 7). In short, we use a modified Mao-Bell type diamond cell to compress samples to the megabar ( $10^{11}$  pascal = 100 GPa) pressure range (8). Pressure is determined at ambient temperature, prior to laser heating, by way of the ruby-fluorescence technique (9). After heating, the pressure is invariably found to be reduced by  $\sim 1$  to 5 GPa. This decrease in pressure is consistent with stress relaxation caused by laser heating, and the pressure before heating is considered to closely approximate the value achieved during heating (6). A continuous (cw) Nd:YAG laser, operating in the fundamental TEM<sub>00</sub> mode ( $\sim 20$  to 25 W output at a wavelength of 1064 nm), is used to heat samples inside the high-pressure diamond cell, and temperatures are measured by spectroradiometry. Our spectroradiometer records the black body-like thermal radiation from the sample at wavelengths between 600 and 800 nm, such that the temperature, and both the spatial variation and uncertainty of the temperature, can be measured between about 1000 and 8000 K (6).

Samples for the present experiments consisted of pure, polycrystalline Pb (10), compacted to a lenticular shape (typical dimensions of  $\sim 80$ - $\mu\text{m}$  diameter and 10- $\mu\text{m}$  maximum thickness), and surrounded by fine-grained ruby that acts both as a refractory container between the diamonds and as a pressure calibrant (7). Below 2000 to 2500 K, the presence of melt could be unambiguously observed in situ during laser heating. Because of the intense thermal radiation emitted at higher temperatures, changes in the surface texture of the sample were used as the criterion of whether or not melting occurred above 2000 to 2500 K (7). The textural observations were carried out at 300 K, after the heating laser had been turned off but while the sample was still under high pressure. At pressures below 30 to 40 GPa, for which the melting temperature is sufficiently low, the textural criterion was found to be in complete agreement with the direct observation of whether melting had occurred or not. Samples were heated for durations of 3 to 30 minutes, with no evidence being found for time dependence in the results or for the sample reacting with the ruby pressure medium [compare with the results of Knittle and Jeanloz (11)].

B. K. Godwal, C. Meade, and R. Jeanloz are in the Department of Geology and Geophysics, University of California, Berkeley, CA 94720. A. Garcia, A. Y. Liu, and M. L. Cohen are in the Department of Physics, University of California, Berkeley, CA 94720, and in the Materials and Chemical Sciences Division, Lawrence Berkeley Laboratory, Berkeley, CA 94720.

\*Permanent address: Neutron Physics Division, Bhabha Atomic Research Center, Trombay, Bombay 400 085, India.

†To whom correspondence should be addressed.

The results of over 200 experimental runs on four different samples of lead are summarized in Fig. 1. The melting temperature is bracketed from above and below at pressures ranging from 9.6 ( $\pm 1.0$ ) to 97.0 ( $\pm 3.2$ ) GPa, and we show bounds determined only with the results from samples that had unambiguously melted or not melted. It is important to note that the bracketing temperatures

represent the peak temperatures achieved in the crystalline or molten Pb at each pressure. Because temperature varies greatly across samples within the internally heated diamond cell, it is necessary to measure profiles of temperature across the heated zone (6, 7, 12). Ten such profiles were determined and used to relate peak temperature with the average sample temperature that is routinely measured in our experiments (13). An example of a temperature profile is shown in Fig. 1.

Two distinct regions are evident in several of our temperature profiles: an inner, high-temperature zone that is characterized by a steep temperature gradient, surrounded by a cooler zone across which temperature varies less rapidly with radial distance. We found the inner zones to extend about 2 to 7  $\mu\text{m}$  from the center of the laser focus (diameters of  $\sim 4$  to 14  $\mu\text{m}$ ), as illustrated by the profile in Fig. 1. Our interpretation is that the change in temperature gradients is attributable to the liquid and solid phases having markedly different physical properties (a combination of optical absorption at the laser wavelength and thermal conductivity) (12). Thus, we infer that the change in temperature gradient occurs at the liquid-solid interface. This conclusion is supported by our observation that the molten zones formed inside the diamond cell (identified either texturally or by direct observation of the melt, in situ) are comparable in dimension to the regions of steep temperature gradients. Furthermore, the five solid-liquid equilibrium temperatures obtained from such profiles, at pressures of 10 to 50 GPa, are in agreement with our melting curve obtained by bracketing (Fig. 1). The beauty of the profiles, however, is that they represent a reversal of the melting transition in a single experiment, thereby yielding a direct measurement of the true equilibrium temperature of fusion.

To check the reliability of our experiments, we compare our results with the melting temperature of lead obtained using other high-pressure techniques. The agreement with the outcome of piston-cylinder experiments is excellent, although the comparison is only possible to 6 GPa (Fig. 1) (14). As our measurements extend the previous determinations of the melting curve of lead by over 15-fold in pressure, we consider the results of shock experiments in the 10 to 100 GPa range. A detailed analysis of the shock-wave equation of state (the Hugoniot curve) has been interpreted as showing that lead melts between 50 and 62 GPa under shock loading (15). More recent measurements of the sound velocity in shock-compressed Pb confirm that melting begins at or below 54 GPa along the Hugoniot (16). Hugoniot temperatures have not been measured for lead, however, so we must turn to theoretical calculations in order to compare our diamond-cell results with the shock-wave data.

**Quantum mechanical calculations.** We have used two first principles quantum mechanical techniques to calculate the energy of crystalline Pb as a function of volume compression. These are the ab initio pseudopotential method (17) and the linear muffin-tin orbitals (LMTO) method (18). Our pseudopotential calculations show that the internal energy and equation of state of the face-centered cubic (fcc) and hexagonal close-packed (hcp) structures of lead are nearly indistinguishable and that we can safely ignore the distinction between these two phases for the present purposes. Both LMTO and pseudopotential calculations include vibrational and electronic contributions to the pressure at finite temperature, so that a direct comparison with experimental data is possible. As explained elsewhere, a Debye-Grüneisen model is used for the thermal corrections and the Hugoniot conservation relations are used to calculate the pressure-temperature-volume conditions achieved upon shock compression (19). Finally, effective interatomic potentials are derived from the crystal energy calculations and used to simulate the equation of state of liquid Pb at high pressures by means of the corrected rigid ion sphere model (20).

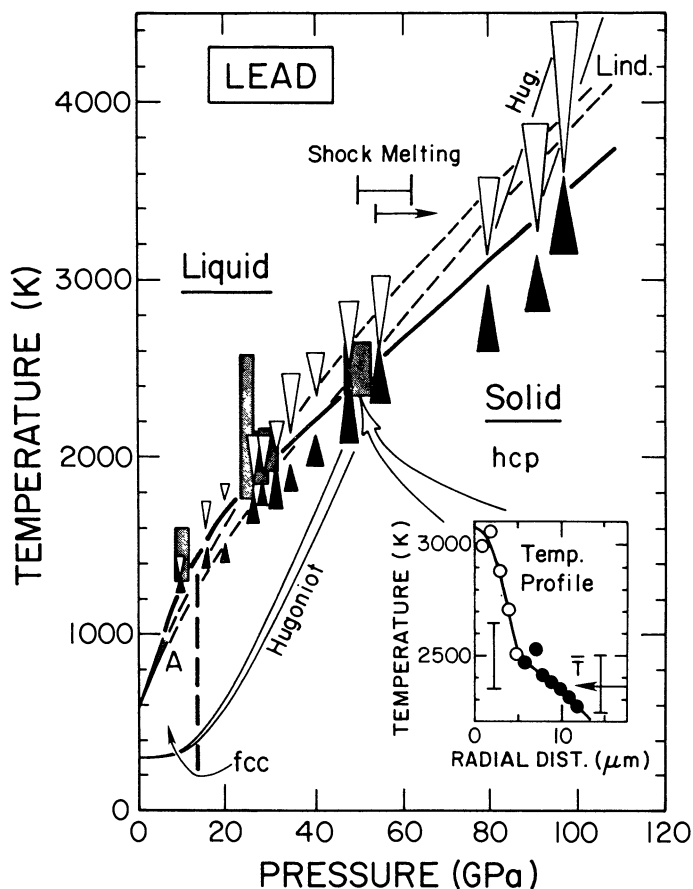


**Fig. 1.** High-pressure melting curve of lead (bold solid line) as determined by experiments with the laser-heated diamond cell: the triangles are brackets on the melting temperature (solid, highest temperature achieved without melting; open, lowest temperature achieved with melt present) and the shaded rectangles indicate temperatures at which the measured profiles exhibit a break in slope. Experiments at temperatures above or below the bracketing values are not shown, and the sizes of the symbols (triangles and rectangles) denote estimates of the uncertainties in pressure and temperature for the runs that are shown (6, 9, 13). The previously determined melting curve [piston-cylinder experiments: curve labeled A (14)] is denoted by shading to 6 GPa, and the transition pressure between face-centered cubic (fcc) and hexagonal close packed (hcp) forms of Pb is given by the bold dashed line (25). The thin solid curves (labeled "Hugoniot" for crystalline lead and "Hug." for liquid lead) show the Hugoniot temperatures computed from the two theoretical methods used in our study: the higher temperature curves are obtained from the pseudopotential calculations and the lower temperature curves are obtained from the LMTO calculations. For comparison, the bracket at 50 to 62 GPa denotes the pressure range over which lead is inferred to melt under shock compression (15); the accompanying arrow summarizes the results of sound velocity measurements demonstrating that lead is molten above 54 GPa along the Hugoniot (16). The thin dashed curves (labeled "Lind.") indicate the melting temperatures predicted from the Lindemann criterion (higher and lower temperature curves obtained from the pseudopotential and LMTO calculations, respectively). (Inset.) A temperature profile measured at 50 ( $\pm 3$ ) GPa: temperature versus radial distance away from the center of the laser focus is given by the circles that have been fitted by two Gaussian profiles, as illustrated (open and closed symbols, interpreted as molten and crystalline lead) (6, 7, 12). The average temperature and its uncertainty ( $T = 2360 \pm 123$  K) and the temperature of the solid-liquid interface ( $2500 \pm 150$  K) are shown for reference (6).

**Table 1.** Calculated and observed equilibrium properties of fcc Pb [at  $T = 300$  K,  $P = 0$ ; experimental data taken from (21, 24)].

| Property                            | Theory                 |             | Experiment           |
|-------------------------------------|------------------------|-------------|----------------------|
|                                     | <i>Pseudopotential</i> | <i>LMTO</i> |                      |
| Volume (cm <sup>3</sup> /mol)       | 18.29                  | 18.18       | 18.27 ( $\pm 0.01$ ) |
| Bulk modulus (GPa)                  | 47.5                   | 49.1        | 44.8 ( $\pm 0.1$ )   |
| Pressure derivative of bulk modulus | 4.0                    | 4.5         | 5.5 ( $\pm 0.1$ )    |
| Debye temperature (K)               | 99                     | 100         | 105 ( $\pm 5$ )      |
| Grüneisen parameter                 | 1.8                    | 2.0         | 2.4 ( $\pm 0.2$ )    |

The Hugoniot temperatures obtained from our theoretical calculations are shown in Fig. 1. Before discussing these results, we point out that the two quantum mechanical techniques yield nearly identical equations of state (the calculated static-lattice isotherms and Hugoniot curves both differ by less than 7.5 GPa at 100 GPa). Also, the results of the two methods are in good agreement with the experimental Hugoniot curve, in accord with what we have found in previous comparisons of these methods with high-pressure experimental data (19). Finally, the reliability of the theoretical calculations is illustrated by the fact that they closely reproduce the ambient condition properties of lead, as summarized in Table 1 (21). This agreement between two of the leading theoretical methods of calculating high-pressure properties of crystals, and between the theoretical results and experimental measurements, is notable in its own right.

Comparing the theoretically calculated Hugoniot temperatures with our experimental melting curve (Fig. 1), we find that lead would be expected to melt upon shock compression to 53 ( $\pm 3$ ) GPa, in complete agreement with the Hugoniot sound velocity and equation of state measurements (15, 16). The mixed phase region of crystals plus melt is expected to extend to 80 to 90 GPa along the Hugoniot, according to our calculations, and this appears to disagree with the value of 62 GPa derived from the experimental Hugoniot (15). If so, the disagreement simply reflects the approximate nature of the liquid state model that we have used (20). In contrast, the agreement between the two theoretical calculations of Hugoniot temperatures for crystalline lead is excellent, as is the agreement between the predicted and observed initiation of melting along the Hugoniot. The consistency that we find lends strong support to the reliability of the laser-heated diamond cell in yielding quantitative determinations of melting temperatures at high pressures.

A well-known model of fusion, often referred to as the Lindemann criterion, assumes that the temperature at which a crystal melts is established by an average of the vibrational amplitudes of the atoms reaching a critical value (3). This model has played an important role in predicting the melting temperatures of materials at high pressures, yet it has rarely been possible to check its reliability over a wide range of pressures. Using our theoretical isotherms and the Debye-Grüneisen model, but no adjustable parameters, we have calculated the melting curve of lead according to the Lindemann criterion (Fig. 1) (19). Although the Lindemann theory yields a melting curve that deviates slightly from our preferred values for lead, the agreement is well within the uncertainty of our data up to the 100-GPa range: a pressure of more than twice the value of the zero pressure bulk modulus. We believe this to be the largest pressure interval over which the Lindemann law has been shown to agree with the experimental measurement of a melting curve. We caution that this agreement may not be general, however, especially for materials with more complex structural or bonding properties than elemental Pb (2, 7, 22).

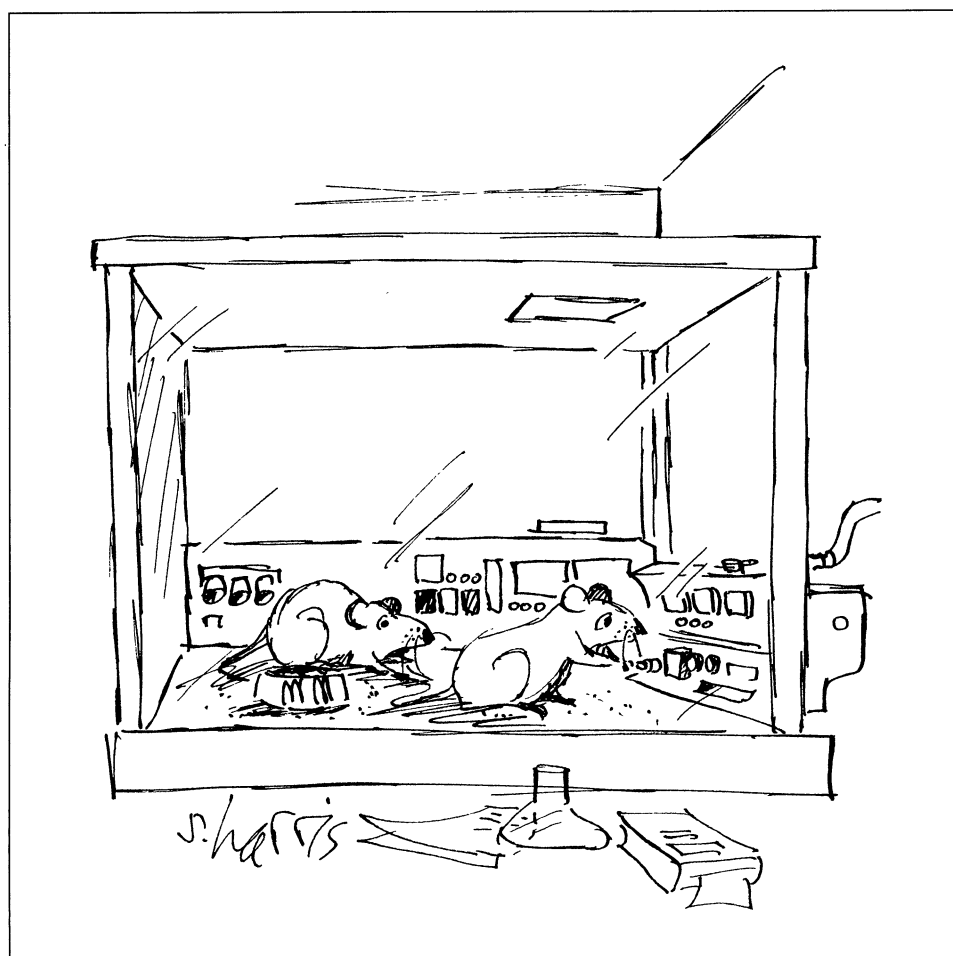
The success of several experimental and theoretical techniques in

determining the high-pressure melting curve of lead suggests that this material would make a good standard for ultrahigh pressure-temperature experiments. Well-calibrated melting experiments at high pressures are especially important for advancing our understanding of how planetary interiors evolve geologically (2, 4, 23). The advantages noted above for considering lead, including the rapid increase of the melting temperature over the pressure interval 0 to 100 GPa, are confirmed by our study. We have presented a melting curve that has been determined over a pressure range extending from far below to well beyond the Hugoniot melting point. Further refinements of our experiments would provide a stringent test of the Lindemann theory of melting; narrowing the present bounds on the melting temperature at 100 GPa would be especially important in this regard. Similarly, measurements of the Hugoniot temperatures achieved in solid and liquid Pb would yield a powerful and independent test of our present results [see, for example (7)]. Hugoniot temperatures for molten lead, in particular, would significantly help improve the current capability in modeling liquid state properties at high pressures.

## REFERENCES AND NOTES

1. J. R. Carruthers, in *Treatise on Solid State Chemistry*, N. B. Hannay, Ed. (Plenum, New York, 1975), vol. 5, pp. 325–406.
2. *Basaltic Volcanism Study Project* (Pergamon, New York, 1981); E. Stolper, D. Walker, B. H. Hager, J. F. Hays, *J. Geophys. Res.* **86**, 6261 (1981); S. M. Rigden, T. J. Ahrens, E. M. Stolper, *Science* **226**, 1071 (1984); Q. Williams and R. Jeanloz, *ibid.* **239**, 902 (1988); C. Meade and R. Jeanloz, *ibid.* **241**, 1072 (1988); E. Knittle and R. Jeanloz, *Geophys. Res. Lett.* **16**, 421 (1989).
3. S. M. Stishov, *Sov. Phys. Uspekhi* **11**, 816 (1969); *ibid.* **31**, 52 (1988); A. R. Ubbelohde, *The Molten State of Matter* (Wiley, New York, 1978); J. M. Ziman, *Models of Disorder* (Cambridge Univ. Press, Cambridge, 1979); G. Venkataraman, D. Sahoo, V. Balakrishnan, *Beyond the Crystalline State* (Springer-Verlag, Berlin, 1989); J. L. Tallon, *Nature* **342**, 658 (1989).
4. R. Jeanloz, *Annu. Rev. Phys. Chem.* **40**, 237 (1989).
5. J. E. Cannon, *J. Phys. Chem. Ref. Data* **3**, 781 (1974); C. W. F. T. Pistorius, *Prog. Solid State Chem.* **11**, 1 (1976); S. P. Marsh, Ed., *LASL Shock Hugoniot Data* (Univ. of California Press, Berkeley, CA, 1980); L. G. Liu and W. A. Bassett, *Elements, Oxides, Silicates* (Oxford Univ. Press, New York, 1986); W. J. Nellis et al., *Phys. Rev. Lett.* **60**, 1414 (1988).
6. D. L. Heinz and R. Jeanloz, in *High-Pressure Research in Mineral Physics*, M. H. Manghanani and Y. Syono, Eds. (American Geophysical Union, Washington, DC, 1987), pp. 113–127; *J. Geophys. Res.* **92**, 11437 (1987). As described in these references and (7), the quoted uncertainties in temperature are estimated standard errors derived from the weighted least-squares fits of either the grey-body spectrum (for an individual measurement of average temperature) or the tomographically deduced temperature profile.
7. Q. Williams et al., *Science* **236**, 181 (1987); Q. Williams, E. Knittle, R. Jeanloz, *J. Geophys. Res.*, in press.
8. H. K. Mao et al., *Rev. Sci. Instrum.* **50**, 1002 (1979).
9. H. K. Mao et al., *J. Appl. Phys.* **49**, 3276 (1978). In the present work, average pressures are quoted with uncertainties representing the range of pressures actually measured. The pressure is measured with a precision better than 0.1 GPa, using our fluorescence system [Q. Williams and R. Jeanloz, *Phys. Rev. B* **31**, 7449 (1985)], whereas the ruby fluorescence shift is calibrated to better than 5% with respect to pressure [H. K. Mao et al., this reference; D. L. Heinz and R. Jeanloz, *J. Appl. Phys.* **55**, 885 (1984)].
10. Obtained from Alpha-Ventron Corp., Danvers, MA, with 99.9999% purity.
11. E. Knittle and R. Jeanloz, *Geophys. Res. Lett.* **16**, 609 (1989).
12. S. Bodea and R. Jeanloz, *J. Appl. Phys.* **65**, 4688 (1989).
13. According to our measurements, the peak temperature ( $T_0$ ) of Pb inside the laser-heated diamond cell is given in terms of the average temperature ( $\bar{T}$ ) by  $T_0$  (K) =  $A + B(\bar{T} - 2000$  K) with  $A = 2509$  ( $\pm 93$ ) K and  $B = 1.32$  ( $\pm 0.21$ ) for  $1000$  K  $< \bar{T} < 3000$  K (the uncertainties represent standard errors from the weighted least-squares fit). This relation is extrapolated to  $\bar{T} \leq 3500$  K in reducing the data from our highest pressure runs. We have included the “fluctuation correction” of previous work (6) into the relation between average and peak temperatures.
14. J. Akella, J. Ganguly, R. Grover, G. Kennedy, *J. Phys. Chem. Solids* **34**, 631 (1973). Considerations of free energy, equivalent to applying Schreinemaker’s rules, demonstrate that the pressure dependence of the melting temperature must be greater above the fcc-hcp-liquid triple point than below the triple point [L. S. Darken and R. W. Gurry, *Physical Chemistry of Metals* (McGraw-Hill, New York, 1953), p. 309].
15. H. Bernier and P. Lalle, in *High Pressure in Research and Industry*, C. M. Backman, T. Johansson, L. Tegnér, Eds. (Arkitektöppa, Uppsala, 1982), vol. 1, pp. 194–197.
16. D. A. Boness, J. M. Brown, J. W. Shaner, in *Shock Waves in Condensed Matter 1987*, S. C. Schmidt, N. C. Holmes, Eds. (Elsevier, New York, 1988), pp. 115–118.
17. M. L. Cohen, *Phys. Scr. T* **1**, 5 (1982); *Science* **234**, 549 (1986).

18. H. L. Skriver, *The LMTO Method* (Springer-Verlag, Berlin, 1984). Both the pseudopotential and the LMTO calculations include scalar relativistic corrections; the spin-orbit interaction that is omitted appears not to affect the static properties [see L. Kleinman, *Phys. Rev. B* **21**, 2630 (1980)].
19. E. Knittle, R. M. Wentzcovitch, R. Jeanloz, M. L. Cohen, *Nature* **337**, 349 (1989); B. K. Godwal and R. Jeanloz, *Phys. Rev. B* **40**, 7501 (1989); *ibid.*, in press.
20. G. I. Kerley, *J. Chem. Phys.* **73**, 469 (1980); *ibid.*, p. 478.
21. Further details are given in B. K. Godwal *et al.*, in preparation.
22. G. H. Wolf and R. Jeanloz, *J. Geophys. Res.* **89**, 7821 (1984).
23. R. Jeanloz and S. Morris, *Ann. Rev. Earth Planet. Sci.* **14**, 377 (1986); R. Jeanloz, *ibid.*, in press.
24. G. Simmons and H. Wang, *Single Crystal Elastic Constants and Calculated Aggregate Properties: A Handbook* (MIT Press, Cambridge, MA, ed. 2, 1971); D. E. Gray, Coordinating Ed., *American Institute of Physics Handbook* (McGraw-Hill, New York, ed. 3, 1972). Uncertainties listed in Table 1 are estimated standard errors reflecting the precision of individual measurements and the range of published values. Note that there is a trade-off between the theoretically derived bulk modulus and its pressure derivative, depending on the way in which the computed results are fitted: decreasing (increasing) the former causes the latter to decrease (increase) [see (19) and A. Garcia, A. Y. Liu, M. L. Cohen, B. K. Godwal, R. Jeanloz, in preparation].
25. T. Takahashi, H. K. Mao, W. A. Bassett, *Science* **165**, 1352 (1969); H. K. Mao and P. M. Bell, *Carnegie Inst. Washington Yearb.* **77**, 842 (1978).
26. We thank E. Knittle, M. Kruger, W. J. Nellis, B. O'Neill, and Q. Williams for helpful discussions. This work was supported by NASA (B.K.G., C.M., and R.J.), and by the National Science Foundation and Department of Energy (A.G., A.Y.L., and M.L.C.). Cray computer time at the NMFEC was provided by the Department of Energy.



"If we didn't do so well in the easy box, they wouldn't have given us this complicated box."